

## Mechanism of Interstitial Oxygen Diffusion in Hafnia

A. S. Foster,<sup>1</sup> A. L. Shluger,<sup>2</sup> and R. M. Nieminen<sup>1</sup>

<sup>1</sup>*Laboratory of Physics, Helsinki University of Technology, P.O. Box 1100, 02015, Finland*

<sup>2</sup>*Department of Physics and Astronomy, University College London, Gower Street, London WC1E 6BT, United Kingdom*

(Received 9 August 2002; published 12 November 2002)

We have performed density functional calculations of oxygen incorporation and diffusion in monoclinic hafnia (HfO<sub>2</sub>) for a range of oxygen charge states. The calculations demonstrate that oxygen favors atomic incorporation and that O<sup>2-</sup> is the most stable species. We find that oxygen interstitials diffuse via exchange with lattice oxygen sites in hafnia, and that O<sup>-</sup> species have the smallest diffusion barrier.

DOI: 10.1103/PhysRevLett.89.225901

PACS numbers: 66.30.Dn, 61.50.Ah, 61.72.-y, 66.30.Jt

Hafnia (HfO<sub>2</sub>) is a wide band gap material, with a high dielectric constant, which has wide applications, especially in optical and protective coating technology [1,2]. The properties of hafnia are also very similar to zirconia due to their homologous electronic outer shell configuration. Both zirconia- and hafnia-related research has received a recent boost due to their possible role in replacing silicon dioxide as the gate dielectric in micro-electronic devices [3]. Thin zirconia and hafnia films deposited on silicon have demonstrated favorable properties in experiments [4–6], such as high thermal stability and low leakage current. Despite this current focus, many of the properties of zirconia and hafnia remain unknown, especially with regard to defect processes. Annealing of films is an intrinsic part of any growth cycle and involves oxygen diffusion through the oxide, as well as the possible formation of interstitial oxygen. However, basic issues, such as the nature of the diffusing oxygen species and the diffusion mechanism, remain unknown. Experiments on zirconia [7,8] have suggested that oxygen incorporates and diffuses in atomic form. Once incorporated, the oxygen can act as an electron trap, changing its charge state and, therefore, its properties and interactions with the oxide and other defects. The performance of thin films in devices is likely to be strongly influenced by these defect processes. In this paper we focus on hafnia in calculations, but its nearly identical physical and electronic structures mean that the results are generally applicable to zirconia as well.

Hafnia exists in three polymorphs at atmospheric pressure: at low temperatures the monoclinic  $C_{2h}^5$  phase (space group  $P2_1/c$ ), above 2000 K the tetragonal  $D_{4h}^{15}$  ( $P4_2/nmc$ ) phase, and above 2870 K the cubic fluorite  $O_h^5$  ( $Fm\bar{3}m$ ) phase. We limit ourselves to the monoclinic structure in this study since it is the most stable phase, even for thin films [9–11]. The monoclinic structure is characterized by three- and four-coordinated lattice oxygen sites, which both could potentially act as defect sites. However, previous studies of monoclinic zirconia and hafnia [12,13] have demonstrated that the reduced space around the four-coordinated sites increases interstitial

defect formation energies. Hence in this work we focus on the more stable three-coordinated defect sites.

All the calculations have been performed using the plane wave basis VASP code [14,15], implementing spin-polarized density functional theory and the generalized gradient approximation (GGA) of Perdew and Wang [16] known as GGA-II. We have used ultrasoft Vanderbilt pseudopotentials [17,18] to represent the core electrons. The pseudopotential for the hafnium atom was generated in the electron configuration  $[\text{Xe} 4f^{14}]5d^3 6s^1$  and that for the oxygen atom in  $[1s^2]2s^2 2p^4$ , where the core electron configurations are shown in square brackets. This method has previously been shown to give excellent agreement with experiment for bulk hafnium and hafnia properties [13] and is well suited for studying defects in this class of materials [12,13].

All calculations were made using a 96 atom unit cell, which is generated by extending the 12 atom monoclinic unit cell by two in three dimensions. For this cell, the total energy was converged for a plane wave cutoff of 400 eV and 2  $k$  points in the first Brillouin zone. One oxygen atom was added to this cell to model the interstitial defect, with a neutralizing background applied for calculations of charged defects. The large size of the cell separates the periodic defect images by over 10 Å, keeping the Coulomb interaction between charged defects in different periodic cells to below 0.1 eV [13]. The diffusion paths were calculated in a static approximation using the nudged elastic band method [19,20].

The incorporation energy of oxygen into the hafnia lattice can be calculated with respect to different processes involving different gas oxygen species [13]. If we consider the case where oxygen incorporates from a molecular source, we find defect energies of +1.6 eV for incorporation of atomic oxygen and +4.2 eV for molecular oxygen, favoring incorporation of two atoms over one molecule by 1 eV. However, for incorporation from an atomic source, such as in ultraviolet ozone oxidation processes (see, for example, [21]), the defect energy for atomic incorporation drops to -1.3 eV, and it is now favored over molecular incorporation by almost 7 eV. In

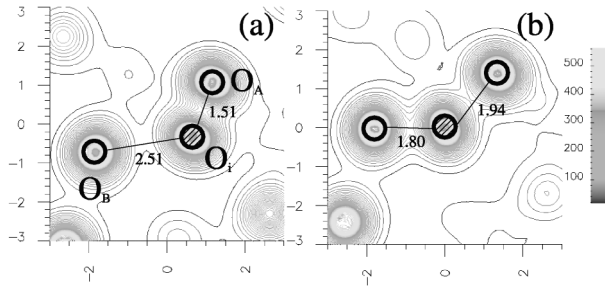


FIG. 1. Charge density plots for neutral interstitial oxygen ( $O_i$ ) in a plane through  $O_A$ ,  $O_i$ , and  $O_B$  for (a) equilibrium geometry near a lattice oxygen ( $O_A$ ), and (b) transition state during exchange diffusion from  $O_A$  to equivalent lattice oxygen site ( $O_B$ ). Charge density is in  $0.1 e/\text{\AA}^3$  and all distances are in  $\text{\AA}$ .

both cases, it is clear that oxygen prefers to incorporate in an atomic form. This agrees with experimental results for similarly structured zirconia [7], and contrasts with the much more open silica structure where molecular incorporation is favored [22].

Figure 1(a) shows a slice of the charge density through the neutral oxygen interstitial and original three-coordinated site. The defect forms a strong bond with lattice oxygen, since this is the closest source of electrons in the system, forming a negatively charged defect pair. Neutral oxygen cannot stably sit isolated in hafnia due to the crystal's high ionicity, and the crystalline potential forces it to a position where it can gain as much charge as possible.

As discussed previously, charge transfer between defects and the oxide/silicon conduction bands, and between defects themselves, has serious implications for device fabrication. Electron trapping from the conduction band is characterized by electron affinities. For defects in hafnia these have been studied in detail previously [13], and therefore here we discuss only those properties relevant to atomic oxygen interstitials. Table I shows that both the neutral and singly charged oxygen interstitials have a large electron affinity and would therefore gain energy by trapping an electron from the conduction band. This is consistent with the efforts of the neutral defect to gain electrons by bonding to the lattice oxygen discussed in the previous section and demonstrates that the ionicity of the crystal energetically favors the existence of oxygen defects as  $O^{2-}$  (negative  $U$  behavior of oxygen is discussed in Refs. [12,13]). Note that in principle the conduction band of hafnia (or silicon for an oxide film on silicon) can always act as a source of electrons, and our calculations predict they will always gain energy by localizing on an oxygen defect. However, studying the actual probability of trapping requires an application of kinetic theory beyond the current scope of this work.

The mechanism of diffusion of oxygen in oxides (and many materials in general) can be classified as occurring via either an exchange or interstitial process. The exchange mechanism [Fig. 2(a)] involves the continuous

TABLE I. Electron affinities ( $\chi_e$ ), exchange activation barriers ( $E_{ex}$ ), and interstitial activation barriers ( $E_{in}$ ) for different charge states of oxygen interstitial defects in hafnia. All values are in eV.

$D$	$\chi_e(D)$	$E_{ex}(D)$	$E_{in}(D)$
$O^0$	3.95	0.8	1.3
$O^-$	4.75	0.3	1.1
$O^{2-}$	...	0.6	1.8

replacement of a lattice site by the diffusing defect, and the lattice site then becoming the diffusing species. This mechanism is traditionally known as the ‘‘Interstitialcy’’ mechanism [23], but we will refer to it as exchange for clarity. It is characteristic of diffusion of anions, for example, in oxides such as  $MgO$  [24] and fluorides such as  $CaF_2$  [25]. In the interstitial mechanism [Fig. 2(b)], the defect diffuses through empty space between the lattice sites. This mechanism is characteristic of diffusion in oxides such as silica [22,26]. The structure of hafnia is more complex than most of these classical cubic oxides, yet retains the same lack of interstitial space, therefore it is especially interesting to see which mechanism is energetically favored. Also in some materials, such as  $MgO$  [24], the mechanism of diffusion is very dependent on the oxygen charge state. The specific barrier for each oxygen species is given in Table I, and in the following sections we discuss in detail the mechanisms themselves.

As discussed previously, the neutral oxygen interstitial in hafnia is characterized by its strong bond with a lattice oxygen site ( $O_A$  in Fig. 1), and we find that it is this need to find an electron source which also dominates the diffusion process. For the exchange mechanism, the transition point occurs when the oxygen atom is more or less equidistant between the initial ( $O_A$ ) and final ( $O_B$ ) lattice

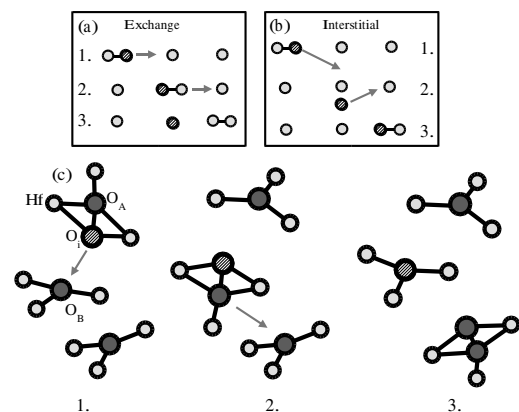


FIG. 2. Schematic diagrams for different diffusion mechanisms: (a) the exchange mechanism for simple cubic lattices, (b) the interstitial mechanism for simple cubic lattices, and (c) the exchange mechanism appropriate to diffusion in hafnia: 1. Initial diffusion of interstitial to nearest lattice oxygen. 2. New defect pair formed, but now lattice oxygen continues diffusion. 3. Interstitial now effectively becomes a lattice site and  $O_B$  diffuses to another lattice oxygen.

oxygen, and the defect is furthest from a source of electrons (the fact that the distances are not exactly equal reflects the asymmetry of the bonding environment around the defect complex in hafnia). Figure 1(b) clearly shows that the defect at this point has much smaller bonding with the lattice sites than in the equilibrium position. The diffusion of the oxygen begins with a reorientation of the oxygen pair, such that the defect moves closer to the final lattice oxygen ( $O_B$ ), but the O-O bond length does not change significantly. After this, the defect moves to the transition state [see Fig. 1(b)], breaking the bond, and then moves almost linearly to bond with the final lattice oxygen. Finally, there is reorientation of the new O-O bond until equilibrium is reached. The energy barrier at the transition state is 0.8 eV.

Diffusion by the interstitial mechanism is in principle governed by similar effects, but traveling between the lattice sites produces a longer path, causes much greater relaxation in the crystal, and causes more difficulty for the defect to bond with lattice sites along the diffusion path. In the exchange mechanism the maximum atom displacement (aside from the diffusing defect itself) is 0.2 Å, with only neighboring oxygen atoms affected. However, for the interstitial mechanism, displacements rise to a maximum of 0.4 Å with both oxygen and hafnium atoms displacing. This is reflected by the increased barrier of 1.3 eV for the interstitial mechanism. Note that due to the increased complexity of the interstitial diffusion path, and the closeness of the exchange and interstitial barriers, the interstitial barrier was checked with double the number of points along the path. This raised the barrier by about 0.1 eV, but did not qualitatively affect the diffusion mechanism.

Introduction of an electron to the system allows the oxygen interstitial to exist more independently from the lattice site, since the electron localizes fully onto the defect. However, the defect is still somewhat coupled to the lattice site with some small covalent bonding evident in Fig. 3(a). However, the diffusion mechanism is simpler than for the neutral case. At first the defect moves linearly in a plane with the initial and final lattice oxygen sites, and there is no reorientation. At the transition point [see Fig. 3(b)], the defect is already almost at its equilibrium bond distance to the final lattice oxygen. However, the final stages of the diffusion involve displacement and reorientation of the new O-O pair to their equilibrium position. The barrier at the transition point is 0.3 eV. Displacement of atoms during the exchange diffusion are of similar magnitude to that for the neutral case, although now more atoms are involved—as to be expected for the increased Coulomb interaction from the charged defect.

The interstitial barrier for the singly charged defect is 1.1 eV, similar to the neutral species, but the comparatively bigger difference to the exchange barrier is due to large displacements along the path. The maximum oxygen displacement is again 0.4 Å, but, as in the exchange

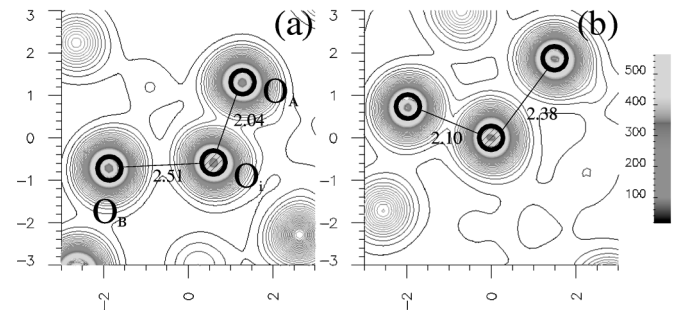


FIG. 3. Charge density plots for singly charged interstitial oxygen ( $O_i$ ) in a plane through  $O_A$ ,  $O_i$ , and  $O_B$  for (a) equilibrium geometry near a lattice oxygen ( $O_A$ ), and (b) transition state during exchange diffusion from  $O_A$  to equivalent lattice oxygen site ( $O_B$ ). Charge density is in  $0.1 e/\text{Å}^3$  and all distances are in Å.

case, the increased Coulomb interaction means that many more atoms are being displaced and the disruption is much more delocalized than for the neutral species.

Adding a second electron to the system effectively creates an independent oxygen with a full outer shell. Figure 4(a) shows that there is now enough extra charge available for the oxygen interstitial to be stable in the crystal without any bonding to the original lattice oxygen sites. This is reflected in both diffusion mechanisms, where the barriers are totally dominated by crystal relaxations due to increased Coulomb interaction. The mechanism is very similar to that for the singly charged defect, with an initial planar diffusion followed by shift of the final oxygen site. However, we see displacements of oxygen atoms slightly larger than that seen for the singly charged defect, and now we also see for the first time significant displacements (over 0.1 Å) of hafnium atoms during exchange diffusion. It is these displacements which give a larger barrier of 0.6 eV for doubly charged diffusion, even though bonding with lattice sites is no longer an issue, and the mechanism is similar to the singly charged case. Figure 4(b) shows that the density configuration of the  $O^{2-}$  defect complex changes little during diffusion, and it is changes in the surrounding atoms that are responsible for the barrier.

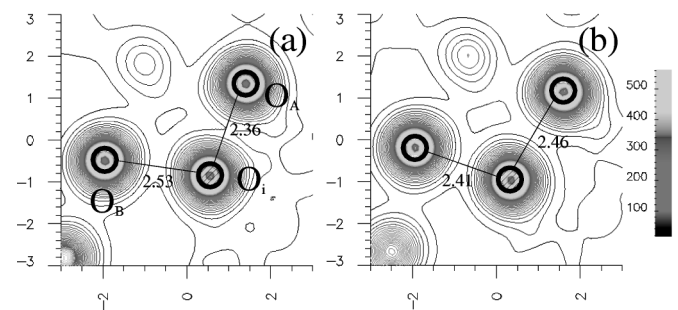


FIG. 4. Charge density plots for doubly charged interstitial oxygen ( $O_i$ ) in a plane through  $O_A$ ,  $O_i$ , and  $O_B$  for (a) equilibrium geometry near a lattice oxygen ( $O_A$ ), and (b) transition state during exchange diffusion. Charge density is in  $0.1 e/\text{Å}^3$  and all distances are in Å.

The doubly charged interstitial diffusion produces the largest relaxations of all the processes, with maximum displacements of over 0.5 Å for surrounding oxygen atoms and up to 0.2 Å for hafnium atoms. This produces a correspondingly large barrier of 1.8 eV.

In summary, oxygen diffusion in hafnia is governed by two competing processes: (i) the crystalline potential in hafnia means that oxygen defects are only stable as ions, and (ii) relaxation of atoms along the diffusion path. The neutral oxygen interstitial causes the least disruption of the surrounding crystal during diffusion, but its need to form an “ion-pair” with a lattice oxygen produces a large barrier. The doubly charged oxygen is the most stable defect in hafnia film on silicon, yet its large Coulomb interaction means it generates large displacements during diffusion. Hence, the singly charged defect proves to be the best balance; it is more independent of the lattice oxygens than the neutral species, but does not produce as large a disruption of the crystal as the doubly charged defect. In terms of the general mechanism, the small space between atoms in hafnia means that the exchange mechanism is favored over the interstitial for all defect species due to the reduction in lattice disruption. Note, however, that in the neutral case, where displacements are in general quite small, the difference between the two mechanisms is much smaller than for the other defect species.

These results show that although hafnia has a much more complex atomic structure than other, simpler ionic materials, its geometry shares a similar lack of interstitial space and the lattice exchange (or interstitialcy) remains the favored diffusion mechanism. In general, the barriers for interstitial oxygen diffusion in hafnia are small, and the defects will be very active, especially during the high temperature processing common in microelectronic processes. These barriers are much smaller than the measured activation energy of 2.3 eV for oxygen diffusion in m-zirconia [8]. However, this activation energy is dominated by the Schottky formation energies (about 2.2 eV [27]). The fact that oxygen is predicted to diffuse as a charged species suggests the possibility of using an applied electric field to influence the diffusion, and perhaps control defect concentrations. The large electron affinity of all the oxygen species means that they can all act as traps within a device, creating intrinsic electric fields and contributing to dielectric losses, so their control would be highly desirable for efficient device design.

This work is supported by the Academy of Finland through its Centres of Excellence Program (2000–2005). A. L. S. is grateful to the EU HIKE project for funding. The authors thank Y.-J. Lee, J. Harding, A. M. Stoneham, A. Korkin, and J. Gavartin for useful discussions. The *lev00* code [28] was used for calculation of density maps.

- [1] J. Wang, H. P. Li, and R. Stevens, *J. Mater. Sci.* **27**, 5397 (1992).
- [2] A. J. Waldorf, J. A. Dobrowolski, B. T. Sullivan, and L. M. Plante, *Appl. Opt.* **32**, 5583 (1993).
- [3] A. I. Kingon, J. P. Maria, and S. K. Streiffer, *Nature (London)* **406**, 1032 (2000).
- [4] G. D. Wilk, R. M. Wallace, and J. M. Anthony, *Appl. Phys. Lett.* **74**, 2854 (1999).
- [5] B. H. Lee, L. Kang, R. Nieh, W.-J. Qi, and J. C. Lee, *Appl. Phys. Lett.* **76**, 1926 (2000).
- [6] M. Gutowski, J. E. Jaffe, C. L. Liu, M. Stoker, R. I. Hegde, R. S. Rai, and P. J. Tobin, *Appl. Phys. Lett.* **80**, 1897 (2002).
- [7] B. W. Busch, W. H. Schulte, E. Garfunkel, T. Gustafsson, W. Qi, R. Nieh, and J. Lee, *Phys. Rev. B* **62**, R13290 (2000).
- [8] U. Brossman, R. Würschum, U. Södervall, and H.-E. Schaefer, *J. Appl. Phys.* **85**, 7646 (1999).
- [9] M. Balog, M. Schieber, M. Michiman, and S. Patai, *Thin Solid Films* **41**, 247 (1977).
- [10] J. Aarik, A. Aidla, H. Mändar, V. Sammelsberg, and T. Uustare, *J. Cryst. Growth* **220**, 105 (2000).
- [11] D. A. Neumayer and E. Cartier, *J. Appl. Phys.* **90**, 1801 (2001).
- [12] A. S. Foster, V. B. Sulimov, F. L. Gejo, A. L. Shluger, and R. M. Nieminen, *Phys. Rev. B* **64**, 224108 (2001).
- [13] A. S. Foster, F. L. Gejo, A. L. Shluger, and R. M. Nieminen, *Phys. Rev. B* **65**, 174117 (2002).
- [14] G. Kresse and J. Furthmüller, *Comput. Mater. Sci.* **6**, 15 (1996).
- [15] G. Kresse and J. Furthmüller, *Phys. Rev. B* **54**, 11169 (1996).
- [16] J. P. Pedew, J. A. Chevary, S. H. Vosko, K. A. Jackson, M. R. Pederson, D. J. Singh, and C. Fiolhais, *Phys. Rev. B* **46**, 6671 (1992).
- [17] D. Vanderbilt, *Phys. Rev. B* **41**, 7892 (1990).
- [18] G. Kresse and J. Hafner, *J. Phys. Condens. Matter* **6**, 8245 (1994).
- [19] G. Mills, H. Jonsson, and G. K. Schenter, *Surf. Sci.* **324**, 305 (1995).
- [20] *Classical and Quantum Dynamics in Condensed Phase Simulations*, edited by B. J. Berne, G. Ciccotti, and D. F. Coker (World Scientific, London, 1998).
- [21] S. Ramanathan, G. D. Wilk, D. A. Muller, C. M. Park, and P. C. McIntyre, *Appl. Phys. Lett.* **79**, 2621 (2001).
- [22] M. A. Szymanski, A. L. Shluger, and A. M. Stoneham, *Phys. Rev. B* **63**, 224207 (2001).
- [23] A. B. Lidiard, *Handbuch der Physik XX* (Springer-Verlag, Berlin, 1957).
- [24] T. Brudevoll, E. A. Kotomin, and N. E. Christensen, *Phys. Rev. B* **53**, 7731 (1996).
- [25] *Defects in Solids: Modern Techniques*, NATO ICI Series B147, edited by A. V. Chadwick and M. Terenzi (Plenum Press, New York, 1985).
- [26] T. Bakos, S. N. Rashkeev, and S. T. Pantelides, *Phys. Rev. Lett.* **88**, 055508 (2002).
- [27] A. Dwivedi and A. N. Cormack, *Philos. Mag. A* **61**, 1 (1990).
- [28] L. N. Kantorovich, [www.cmmp.ucl.ac.uk/~lev](http://www.cmmp.ucl.ac.uk/~lev) (2001).